

where θ is one-half the scattering angle, λ the final wavelength, λ_0 the initial wavelength, and $\Delta\lambda = \lambda - \lambda_0$. The area under this curve was normalized to ten electrons, i.e., one-half the total number of excited electrons [$2s^2 2p^6 3s^2 3p^6 (3d 4s)^4$]. (The $1s^2$ are too tightly bound to be excited.)

The final normalized profile $J(z)$ is shown in Fig. 1, together with the Compton profiles calculated from Hartree-Fock free-atom wave functions³ for $3d^3 4s$ and $3d^4$ valence-electron configurations. Included also are the calculated core profile ($2s^2 2p^6 3s^2 3p^6$) and the profile in free-electron theory (4 free electrons per atom).

Since the data were taken on a polycrystalline sample, it is a straightforward procedure to determine the spherically averaged momentum density $|\chi|^2$ from the slope of the $J(z)$ curve since¹

$$4\pi|\chi|^2 = |(2/z)(dJ/dz)|. \quad (2)$$

The momentum density is shown in Fig. 2 together with the calculated momentum densities from Hartree-Fock free-atom wave functions for the configurations $3d^3 4s$ and $3d^4$ and that calculated from free-electron theory.

To establish the position of the metallic discontinuity in momentum density (which appears as a discontinuous change in slope in Fig. 1 and a discontinuity in Fig. 2 at $z \cong 1.1$), a large number of additional runs were taken at intervals of 0.000 15 Å over a limited range of wavelengths in the vi-

cinity of the free-electron value of Fermi momentum. The corresponding momentum range examined was approximately 0.7 to 1.5 a.u. The discontinuity in slope was observed at 1.08 ± 0.06 a.u. which is close to the free-electron value of 1.01 a.u. for titanium.

It is interesting that the calculated free-atom Compton profile is so sensitive to the relative 4s and 3d character in the valence band. A shift of one 3d electron to 4s produces over a 30% change in $J(z)$ at $z = 0$ (Fig. 1). Until band calculations for titanium are evaluated in momentum space or the space wave functions transformed to momentum space, no comparison with band theory is possible. Free-electron behavior and free-atom (Hartree-Fock) behavior for the four valence electrons, however, represent the two extremes, and the experimental data lie somewhere between the two. It does appear, though, that something between 0.5 and 1.0 4s electron occupies the band in titanium. The observed structure in the momentum density at $p \sim 0.45$ and $p \sim 0.70$ (Fig. 2) is presumably a solid-state effect.

¹W. C. Phillips and R. J. Weiss, Phys. Rev. **171**, 790 (1968).

²W. A. Rachinger, J. Phys. E: J. Sci. Instr. **25**, 254 (1968).

³R. J. Weiss, W. C. Phillips, and A. Harvey, Phil. Mag. **17**, 146 (1968).

CONFIGURATION COORDINATES OF Tl^+ IN KCl FROM RAMAN SCATTERING

L. C. Kravitz

General Electric Research and Development Center, Schenectady, New York 12301

(Received 18 February 1970)

Raman scattering data for KCl: Tl^+ crystals are reported. The dominant scattering amplitudes are attributed to vibrations having E_g and T_{2g} symmetry about the Tl^+ ion. Comparison of the data with theory suggests a small change in interatomic force constants which can be understood in terms of Coulomb and repulsive forces. The Tl^+ -Cl equilibrium spacing in the electronic ground state appears to be consistent with the value computed by Williams.

Although Seitz¹ had, in 1938, given an essentially correct analysis of the optical absorption bands of Tl^+ in KCl, research interest in this ion continues to the present. As a prototype of a series of ions, including In^+ , Pb^{++} , Sn^{++} , and Sb^{+++} , Tl^+ represents an important class of phosphor sensitizers. In addition, it possesses an electronic simplicity which has made it and continues to make it extremely attractive for fundamental studies.

The ultraviolet absorption bands of Tl^+ are associated with transitions from a 1S_0 ($6s^2$) ground state to the ($6s6p$) manifold of states derived from 1P_1 , 3P_2 , 3P_1 atomic states. The relative widths and intensities of these three bands have been discussed in terms of lattice interactions and spin-orbit splittings, using configuration-coordinate curves to describe the lattice interaction, although the precise nature of the coordinates have, of necessity, been unspecified until

quite recently.

The first such experimental suggestion of configuration coordinates was found by Fukuda² Inohara, and Onaka² for the isoelectronic systems $\text{KCl}:\text{In}^+$ and $\text{KCl}:\text{Sn}^{++}$, in which a temperature-dependent multiplet structure of the absorption bands was observed. This structure was interpreted by Toyozawa and Inoue³ as arising from a dynamic Jahn-Teller effect wherein the excited electronic states are coupled with lattice distortions having T_{2g} symmetry.

Recently⁴ the observation of E_g and T_{2g} vibrational Raman spectra of Tl^+ -doped KBr , KI , and KCl have been reported. These observations on KBr and KI appear to be consistent with a lattice-dynamical theory in which no change of Tl^+-Cl^- force constant is introduced. The agreement for KCl was less positive as certain predicted spectral features were not observed. In the present paper we report Raman spectra of $\text{Tl}^+:\text{KCl}$ which are in good agreement with theoretical spectra including a change in force constant consistent with the model of Williams.⁵

Crystals containing up to 0.60 molar percent Tl were grown by the Bridgman technique in sealed, argon-filled, quartz tubes. The volatile TlCl was thus contained, assuring an ample concentration of Tl in the crystal. The charges of TlCl and Harshaw KCl were fired in flowing HCl prior to sealoff.

The Raman apparatus consisted of an argon laser source, a Spex double monochromator, and an S-11 phototube feeding a recording microammeter.⁶ Measurements at 300°K were made with incident and scattered light polarizations chosen in accord with selection rules

$$(A_{1g} + E_g):(100, 100); \quad E_g:(110, 1\bar{1}0);$$

$$T_{2g}:(100, 010).$$

Experimental data are shown in Fig. 1 for both Stokes and anti-Stokes scattering. The second-order lattice scattering can be observed only on the Stokes side of the $(A_{1g} + E_g)$ spectrum, and is identical to that observed in an undoped, but otherwise identically prepared sample. The relative intensities of the impurity-induced and second-order scattering spectra were found to vary from sample to sample in accord with the chemically determined Tl concentration.

We follow the work of Xinh, Maradudin, and Coldwell-Horsfall⁷ (XMC) who have computed the projected densities of states for both pure and impure KCl lattices. These authors employ the phonon spectra computed by Jaswal and ac-

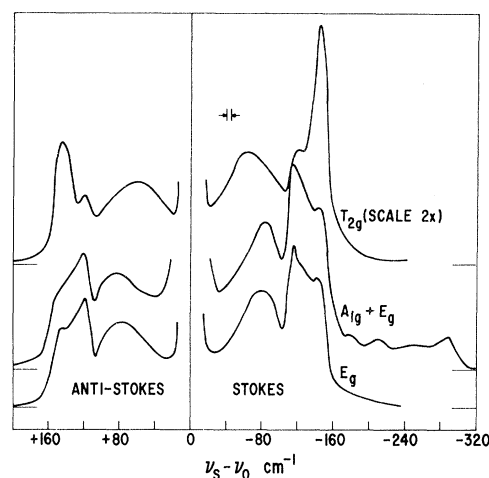


FIG. 1. Raman spectra at 300°K for $\text{KCl}:\text{Tl}$ (0.005). The baselines of the data have been displaced vertically. All measurements were at the same laser power, gain settings, and slit width of 5 cm^{-1} . The peak-signal-to-noise ratio was approximately 20.

count for the defect perturbation of the phonon spectrum by means of the parameters

$$\beta = \omega_L^2 (M_+ M_-)^{-1/2} \Delta \phi_{xx}(01),$$

$$\gamma = \omega_L^2 (M_+ M_-)^{-1/2} \Delta \phi_{yy}(01),$$

where ω_L is the maximum frequency of the unperturbed lattice, and $\Delta \phi_{xx}(01) = \Phi_{xx}(0, 1, \text{K}) - \Phi_{xx}(0, 1, \text{Tl})$. Here $\Phi_{xx}(0, 1, \text{K})$ is the longitudinal spring constant joining the K^+ site and its near-neighbor Cl^- ion and similarly for Φ_{yy} for the transverse case.

In Figs. 2 and 3 we compare our data with those histograms of XMC which most nearly fit our data. Using their curves, we can estimate that for Tl^+ the values of β and γ are within the limits set by $-0.05 < \beta < 0$ and $-0.05 < \gamma < -0.01$ for $\omega_L = 210 \text{ cm}^{-1}$. This value of β can be compared with one calculated by computing Φ_{xx} on the basis of a Born-Mayer potential of the form $\lambda e^{-r/\rho}$ and a Coulomb interaction. Values of λ and ρ were taken from Born and Huang⁸ for KCl and from Mayer⁹ for TlCl . The Tl^+-Cl^- separation was taken as 0.09 \AA greater than that for K^+-Cl^- in accord with the estimate of Williams. The value of β computed in this way was $\beta = -0.013$, which is within the range of the estimate above.

Although hydrostatic pressure experiments¹⁰ have shown an absorption energy dependence which is linear with A_{1g} distortion, the experimental Raman data of Fig. 1, particularly the strong similarities of $A_{1g} + E_g$ and E_g , do not indicate any interaction between the Tl^+ defect and the A_{1g} breathing mode vibration. Indeed, as

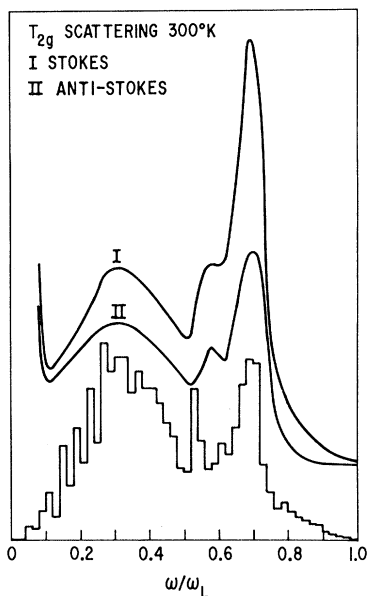


FIG. 2. A comparison of the T_{2g} Raman spectra with the T_{2g} histogram of XMC for $\gamma = -0.01$.

suggested by Toyazawa and Inoue for other heavy metal ions, the important line-broadening interactions appear to be with those asymmetric vibrations capable of lifting the degeneracies of the excited states. A contribution to the Raman cross section also results from a modulation of the off-diagonal terms of the polarizability tensor by the phonon-induced admixture of p_x and p_y electronic states.

The intensity of scattering for a particular symmetry depends upon the nature of the defect. For example, Hurrell et al.¹¹ have studied $KBr_{1-x}Cl_x$ crystals and have found only A_{1g} vibrational scattering, in contrast to our results where A_{1g} scattering was absent. Our results are thus more closely related to those for the F center in which the asymmetric vibrations were also found to lift the excited-state degeneracy.¹²

The use of Raman scattering to study the lattice vibrational interactions of Tl^+ in KCl has confirmed the theoretical conclusions drawn by Toyazawa and Inoue for other heavy metal ions in that the important local vibrational distortions at the defect site possess symmetries of E_g and T_{2g} . Phonons from acoustic as well as the optical branches contribute to these distortions, the major contribution coming from high-symmetry regions of the Brillouin zone in which $ka \sim \pi/2$.

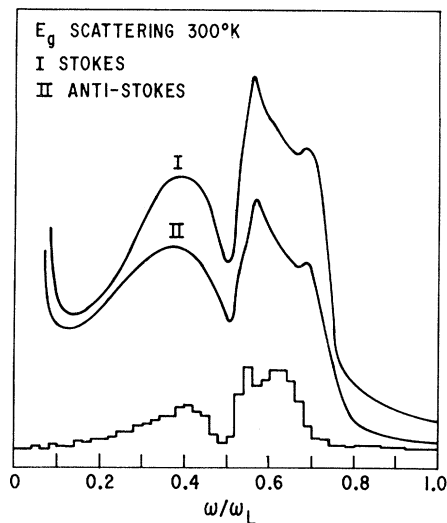


FIG. 3. A comparison of the E_g Raman spectra with the E_g histogram of XMC for $\beta = -0.05$.

Although the spectra are described quite well by the deformation dipole based theory of XMC, a shell-model theory based upon the recent results of Copley, McPherson, and Timusk¹³ might further improve the agreement between theory and experiment.

The assistance of C. R. Trzaskos in the preparation of the crystals is gratefully acknowledged.

¹For a review of the early research see W. B. Fowler, in *Physics of Color Centers*, edited by W. B. Fowler (Academic, New York, 1968).

²A. Fukuda, K. Inohara, and R. Onaka, *J. Phys. Soc. Japan* **19**, 1274 (1964).

³Y. Toyazawa and M. Inoue, *J. Phys. Soc. Japan* **21**, 1663 (1966).

⁴R. T. Harley, J. B. Paige, and C. T. Walker, *Phys. Rev. Letters* **23**, 922 (1969).

⁵F. E. Williams, *J. Chem. Phys.* **19**, 457 (1951).

⁶L. C. Kravitz, J. D. Kingsley, and E. L. Elkin, *J. Chem. Phys.* **49**, 4600 (1968).

⁷N. X. Xinh, A. A. Maradudin, and R. A. Coldwell-Horsfall, *J. Phys. (Paris)* **26**, 717 (1965).

⁸M. Born and K. Huang, *Dynamical Theory of Crystal Lattices* (Oxford Univ., Oxford, England, 1954).

⁹J. E. Mayer, *J. Chem. Phys.* **1**, 327 (1933).

¹⁰P. B. Alers and P. E. V. Shannon, *J. Chem. Phys.* **41**, 1675 (1964).

¹¹J. P. Hurrell, S. P. S. Porto, T. C. Damen, and S. Mascarenhas, *Phys. Letters* **26A**, 194 (1968).

¹²See article by C. H. Henry in Ref. 1.

¹³J. R. D. Copley, R. W. McPherson, and T. Timusk, *Phys. Rev.* **182**, 965 (1969).